



Reply to Comment on “*Aysheaia prolata* from the Utah Wheeler Formation (Drumian, Cambrian) is a frontal appendage of the radiodontan *Stanleycaris*” with the formal description of *Stanleycaris*

STEPHEN PATES, ALLISON C. DALEY, and JAVIER ORTEGA-HERNÁNDEZ

As part of a comprehensive examination of all radiodontans from Cambrian localities in the USA, Pates et al. (2017a, b) and Pates and Daley (2017) revised the taxonomic affinities of several described specimens. This included the reinterpretation of two putative lobopodians, one from the Wheeler Formation (Utah, USA) and one from the Valdemiedes Formation (Spain), as frontal appendages of the radiodontan genera *Stanleycaris* and *Caryosyntrips* respectively. In their comment, Gámez Vintaned and Zhuravlev (2018) disagree with these conclusions and raise three topics for discussion: (i) anatomical features they suggest support a lobopodian affinity for “*Mureropodia*”; (ii) the identity of *Caryosyntrips* as a radiodontan, and the assignment of certain specimens to this genus; and (iii) the nomenclatural status of *Stanleycaris hirpex* as an invalid taxon. For (i), we dispute that the anatomical features put forward by Gámez Vintaned and Zhuravlev (2018) are biological and conclude that a lobopodian affinity for *Mureropodia* is untenable. In response to (ii), we provide further evidence supporting a radiodontan affinity for *Caryosyntrips*, and those specimens ascribed to this genus. Finally, we concur with (iii) *Stanleycaris* as an invalid taxon according to the International Code on Zoological Nomenclature (ICZN), and have rectified the situation by providing a valid systematic description.

“*Mureropodia*” is not a lobopodian

Gámez Vintaned and Zhuravlev (2018) argue that Pates and Daley (2017) ignored characters supporting a lobopodian affinity for “*Mureropodia*”, such as the musculature, an antenniform appendage, retractable proboscis, claws and transverse telescopic structures. We find that these features consist of diagenetic artefacts, over-interpreted textures from the matrix, or preparation marks.

Musculature.—Based on our examination of the only specimen, the microstructures identified by Gámez Vintaned et al. (2011) as muscles represent abiotic lineations in the rock. These lineations are an order of magnitude larger than previously published muscular fibres in *Pambdelurion* (Gámez Vintaned et al. 2011: 209; see also Budd 1997; Young and Vinther 2017), and

extend beyond the fossil margins into the rock matrix, demonstrating that they are not part of the fossil specimen.

Antenniform frontal appendage.—There are no features that distinguish the structure regarded by Gámez Vintaned et al. (2011) as an antenniform limb, and the interpretation of this feature as a small burrow is more compelling as it extends into the surrounding matrix. Structures identified as “pores” are likely plucked mineral grains approximately aligned in this region, and other unaligned voids can be seen elsewhere in the SEM images (Gámez Vintaned et al. 2011: fig. 12.5h, k).

Proboscis with retractor-protractor muscle system.—The presence of a fleshy proboscis among lobopodians has only been reliably documented in the Chengjiang *Onychodictyon ferox* (Ou et al. 2012). The feature preserved on the anterior end of “*Mureropodia*” bears no morphological resemblance to the former taxon, and as mentioned earlier, structures interpreted as the retractor-protractor muscle system in Gámez Vintaned et al. (2011) are most likely abiotic. The identification of this structure as the distorted distal end of a *Caryosyntrips* appendage is preferred, as similar distortions have been identified in *Caryosyntrips* specimens from the Burgess Shale (Pates and Daley 2017: fig. 4B, D).

Claws.—Structures interpreted as claws by Gámez Vintaned et al. (2011) consist of minute scarps resulting from fossil preparation. These features are indistinguishable from the matrix, whereas lobopodian claws represent heavily sclerotized structures preserved as flattened carbon films (e.g., Smith and Ortega-Hernández 2014: fig. 1a–d; Ortega-Hernández 2015: fig. 1b; Yang et al. 2015: fig. 2b). We thank Gámez-Vintaned and Zhuravlev (2018) for correcting the labelling of fig. 3D in Pates et al. (2017b), which does correspond to *Aysheaia pedunculata*, as this photograph further serves to illustrate the fundamental differences between the distinctive appearance of the sclerotized terminal claws of lobopodian limbs and the features incorrectly interpreted as claws by Gámez Vintaned et al. (2011). We have not interpreted these structures as auxiliary spines, unlike stated by Gámez Vintaned and Zhuravlev (2018), because we are not convinced that they have a biological origin.

Transverse telescopic structures.—The transverse telescopic structures along the putative lobopods are indistinguishable

from the texture and uneven surface relief of the rest of the specimen and the surrounding matrix, and are accentuated by shadows created by low-angle lighting across the fossil surface. The presence of lobopods is further problematic as the putative limbs have a much lower length/body ratio compared to all other Cambrian lobopodians, even smaller than that of *Antennacanthopodia gracilis* from the Chengjiang biota (Ou et al. 2011) or extant onychophorans (Haug et al. 2012). By contrast, the length/width ratio of these features falls comfortably within the range observed in the ventral spines of *Caryosyntrips* appendages (Pates and Daley 2017).

Caryosyntrips is a radiodontan

The criticisms by Gámez Vintaned and Zhuravlev (2018) on the affinities of *Caryosyntrips* are based on numerous incorrect statements and factual errors, compounded by an outdated attempt to use biomechanical and ecological statements to infer phylogenetic relationships, which ultimately have no bearing on resolving the affinities of this taxon.

The (un)importance of θ .—Gámez Vintaned and Zhuravlev (2018) claim the angle between dorsal and ventral surfaces, θ , (Pates and Daley 2017: fig. 2) is an “important character of radiodontan frontal appendages according to Pates et al. (2017b)”. This angle was discussed only in relation to *Caryosyntrips* (Pates and Daley 2017, not Pates et al. 2017b) and was never claimed to be a relevant character for all radiodontan frontal appendages. Thus, θ was included in the description only to quantify the thickness and tapering outline of known *Caryosyntrips* appendages and was not included in the diagnosis of the genus of any of the species, which are based on more robust characters: the presence of large and small dorsal spines; paired ventral spines; terminal spines; a bell-shaped proximal margin; and the presence of podomeres.

***Caryosyntrips* is not a hyolith, poriferan, chancelloriid, or lobopodian.**—Gámez Vintaned and Zhuravlev’s (2018) misunderstanding of the importance of the θ angle led them to draw attention to non-radiodontan taxa with similar sub-conical shapes, namely hyoliths, archaeocyathids, sponges, chancellorids, and lobopodians. Gámez Vintaned and Zhuravlev (2018) argue that the distinctive shape of *Caryosyntrips* appendages contradict its interpretation as a radiodontan, and that its θ angle values of 11–18° support its affinities among these other taxa. This is untenable based on the fundamental morphology of these biomineralized organisms, whose organization consists of calcareous conical shells (hyoliths), cup-shaped carbonate skeletons (archaeocyathids), siliceous or calcareous spicules (sponges), and meshes of star-shaped calcareous spicules (chancellorids), none of which are found in *Caryosyntrips*. Although similar preservation of soft-bodied radiodontan frontal appendages and lobopodians may result in misinterpretation (see Pates et al. 2017b), the available *Caryosyntrips* material lacks any features that would support a lobopodian affinity such as annulations, dorsal sclerites, claws, or a differentiated oral region (Ortega-Hernández 2015).

***Caryosyntrips* is a radiodontan.**—Numerous anatomical features indicate that “*Mureropodia*” and other *Caryosyntrips* specimens represent radiodontan frontal appendages, particularly when taphonomic variability is taken into consideration. The best preserved *Caryosyntrips* specimens from the Burgess Shale reveal the presence of discrete podomeres separated by arthro-dial membranes, a single pair of ventral spines per podomere, dorsal spines, and the distinct distal taper and straight outline of the appendage shape (Pates and Daley 2017: figs. 3A, F, 4A). The more incompletely preserved specimens (Pates and Daley 2017: figs. 3E, 4C, 5) questioned by Gámez Vintaned and Zhuravlev (2018) show numerous features that support a radiodontan affinity, and specifically their similarity to *Caryosyntrips*. These include: traces of the podomere boundaries and arthro-dial membranes (white arrows in Pates and Daley 2017: fig. 4C, E); regular spacing and near-parallel orientation of paired ventral spines (Pates and Daley 2017: figs. 4C, E, 5); circular attachments for, or presence of dorsal spines (Pates and Daley 2017: figs. 3E, 5); and distinct distal tapering (Pates and Daley 2017: figs. 3E, 4C, E, 5). The same logic identifies other poorly preserved *Caryosyntrips* from the Burgess Shale (Pates and Daley 2017: figs. 3B–D, 4B, D, E) not questioned by Gámez Vintaned and Zhuravlev (2018). Gámez Vintaned and Zhuravlev (2018) incorrectly claim “Pates and Daley (2017) thought that *Mureropodia* had to have dorsal spines which were absent due to incomplete preservation of the dorsal surface”. “*Mureropodia*” was left in open nomenclature as *Caryosyntrips* cf. *camurus* (which does not bear dorsal spines—see Pates and Daley 2017: figs. 1, 4) partly because the dorsal surface is too poorly preserved to determine if dorsal spines are truly absent (Pates and Daley 2017: 466). In contrast to the assertion of Gámez Vintaned and Zhuravlev (2018), Radiodonta such as *Hurdia*, *Peytoia*, and *Anomalocaris* possess frontal appendages with hinge-less ventral spines, and so the absence of hinged ventral spines in *Caryosyntrips* adds further evidence to its interpretation as a radiodontan frontal appendage.

Radiodontan frontal appendages can be preserved dorso-ventrally.—Contrary to the claims of Gámez Vintaned and Zhuravlev (2018), radiodontan frontal appendages are regularly buried in various orientations, including obliquely (Daley and Budd 2010: text-fig. 7D; Daley and Edgecombe 2014: figs 12.3, 12.4, 13.2, 13.4, 13.6) and dorsoventrally (Daley and Edgecombe 2014: figs. 4.1, 12.8; Pates et al. 2017a: fig. 3: app. 2). The ventral spines in KUMIP 314275 (Pates and Daley 2017: fig. 4C) are interpreted as appearing on both sides of the distal tip of the appendage because it is preserved at an oblique orientation to the sediment, and so the paired ventral spine appears on the dorsal side due to the thin (sag.) podomeres at the distal end of the appendage. Burgess Shale *Caryosyntrips* appendages ROM 59497 and ROM 59599 similarly show ventral spines just visible on both sides of the thin distal tip of the appendage due to oblique orientation (Pates and Daley 2017: figs. 3F, 4E). An alternate explanation, that large dorsal spines are present in these specimens, does not negate their radiodontan affinity given that prominent distal dorsal spines are known from many representatives of this group, including *Caryosyntrips durus*.

Ecology of *Caryosyntrips*.—Gámez Vintaned and Zhuravlev (2018) use incorrect biomechanical and ecological statements to exclude specific specimens (Pates and Daley 2017: figs. 3E, 4C, 5) and *Caryosyntrips* as a whole from Radiodonta. The Radiodonta have a wide variety of frontal appendage morphologies and distinct ecologies, and not all frontal appendages are equally flexible. *Anomalocaris* and *Amplectobelua* have discrete arthro-dial membranes between the podomeres that would have allowed them to actively grab prey through dorsoventral flexure (Briggs 1979; Hou et al. 1995; Daley and Budd 2010; Daley and Edgecombe 2014), however, triangular arthro-dial membranes are not visible in radiodontans such as *Aegirocassis* and *Hurdia*, and so the podomeres with large endites did not have a high degree of flexure (Daley et al. 2009, 2013; Van Roy et al. 2015). This movement restriction allowed all the large endites to function as a sieve and filter plankton from the water column (*Aegirocassis*) or sift sediment (*Hurdia*). *Caryosyntrips* frontal appendages were not “non-functional”, because they moved in a transverse scissor or slicing motion, pivoting at the bell-shaped basal attachment joint as discussed in detail in Daley and Budd (2010: 734–735) and Pates and Daley (2017: 468). Finally, we must emphasise that functional morphology cannot be used to resolve phylogenetic affinities. The presence and morphology of paired ventral spines, dorsal spines, podomeres, and arthro-dial membrane all support the identification of these *Caryosyntrips* specimens as radiodontan frontal appendages, regardless of function.

Institutional abbreviations.—KUMIP, Division of Invertebrate Paleontology, Biodiversity Institute, University of Kansas, Lawrence, Kansas, USA; ROM, Royal Ontario Museum, Toronto, Canada.

Other abbreviations.—P, podomere; sag., sagittal; trans., transverse.

Nomenclatural acts.—This published work and the nomenclatural acts it contains have been registered in ZooBank, the online registration system for the ICZN. The electronic edition of this work is available from the following digital repository: <http://www.app.pan.pl/article/item/app004432017.html>

Systematic palaeontology

Phylum (total-group) Euarthropoda Lankester, 1904

Order Radiodonta Collins, 1996

Family Hurdiidae Vinther, Stein, Longrich, and Harper, 2014

Genus *Stanleycaris* nov.

ZooBank LSID: urn:lsid:zoobank.org:act:EAEF5A9-FAF4-4423-8EA1-B0F5DF35A4C8

2010 *Stanleycaris* gen. nov.; Caron et al. 2010: 811, 813, supplementary material 5: 8–10, pl. 1 (nomen nudum).

2011 *Stanleycaris* Caron, Gaines, Mángano, Streng, and Daley, 2010; Zamora et al. 2011: 655.

2013 *Stanleycaris* Caron, Gaines, Mángano, Streng, and Daley, 2010; Liu 2013: 338.

2014 *Stanleycaris* Caron, Gaines, Mángano, Streng, and Daley 2010; Vinther et al. 2014: 498, fig. 3.

2015 *Stanleycaris* Caron, Gaines, Mángano, Streng, and Daley 2010; Daley and Legg 2015: 953.

2017 *Stanleycaris* Caron, Gaines, Mángano, Streng, and Daley 2010; Pates et al. 2017: 12–13.

2017 *Stanleycaris* Caron, Gaines, Mángano, Streng, and Daley 2010; Pates and Daley 2017: 468.

2017 *Stanleycaris* Caron, Gaines, Mángano, Streng, and Daley 2010; Pates et al. 2017: 619–622, figs. 1–3.

Etymology: Named for Stanley Glacier (Kootenay National Park) where the material was collected, and from the Latin *caris*, crab.

Type species: *Stanleycaris hirpex* sp. nov., Stephen Formation (Cambrian Series 3, Stage 5) near Stanley Glacier, Kootenay National Park, British Columbia, Canada.

Species included: *Stanleycaris hirpex* and *Stanleycaris* sp.

Diagnosis.—Frontal appendage with 11 distally tapering podomeres; one robust double-pointed or single-pointed spine projects from the dorsal surface of P2–11 either vertically or at an oblique angle; P2–6 bear a spinous ventral blade slightly curved distally 2–3 times the length (sag.) of the height (sag.) of the dorsal spines (adapted from Caron et al. 2010).

Remarks.—As pointed out by Gámez Vintaned and Zhuravlev, the original description of *Stanleycaris* in the online supplementary information of Caron et al. (2010) is not ICZN compliant, as only online descriptions published in 2011 or later are accepted according to the current iteration of the code (ICZN 2012). This contribution formalises *Stanleycaris* as a taxonomically valid scientific name.

Stratigraphic and geographic range.—*Stanleycaris hirpex*, Thin Stephen Formation (Cambrian Series 3, Stage 5), British Columbia, Canada (Caron et al. 2010); *Stanleycaris* sp., Wheeler Formation, House Range (Cambrian Series 3, Drumian), Utah, USA (Pates et al. 2017b).

Stanleycaris hirpex sp. nov.

Figs. 1A–C, 2.

ZooBank LSID: urn:lsid:zoobank.org:act:525F2CD0-FC9F-4E6D-8591-1C942D665D5A

2010 *Stanleycaris hirpex* gen. et sp. nov., Caron et al. 2010: 811, 813, supplementary material 5: 8–10, pl. 1 (nomen nudum).

2011 *Stanleycaris hirpex* Caron, Gaines, Mángano, Streng, and Daley 2010; Gaines 2011: 74.

2014 *Stanleycaris hirpex* Caron, Gaines, Mángano, Streng, and Daley 2010; Vinther et al. 2014: extended data fig. 4.

2014 *Stanleycaris hirpex* Caron, Gaines, Mángano, Streng, and Daley 2010; Cong et al. 2014: extended data fig. 4.

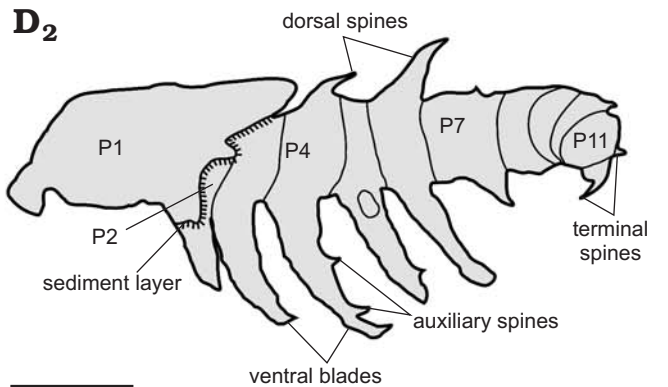
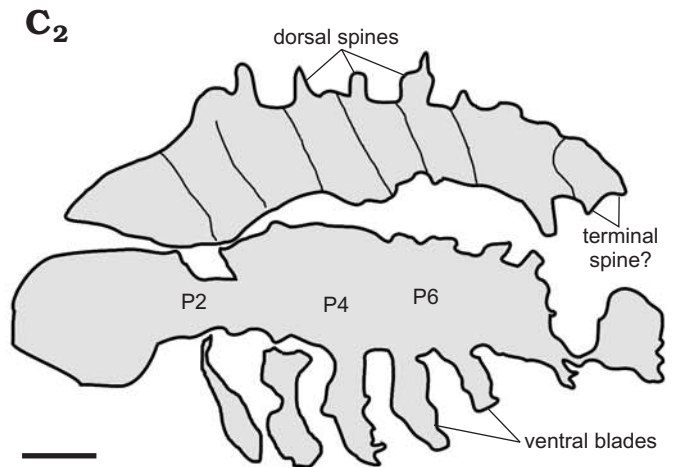
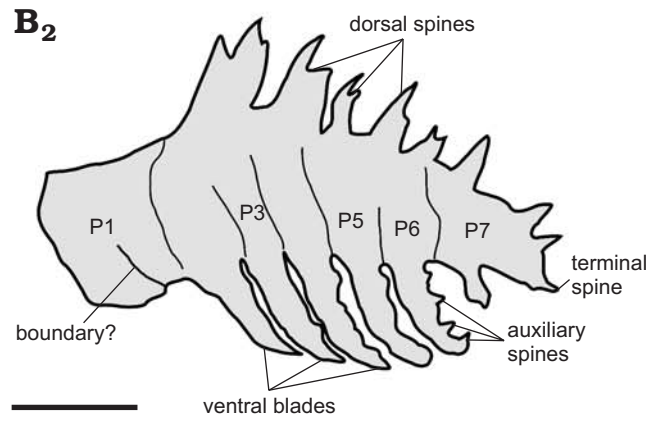
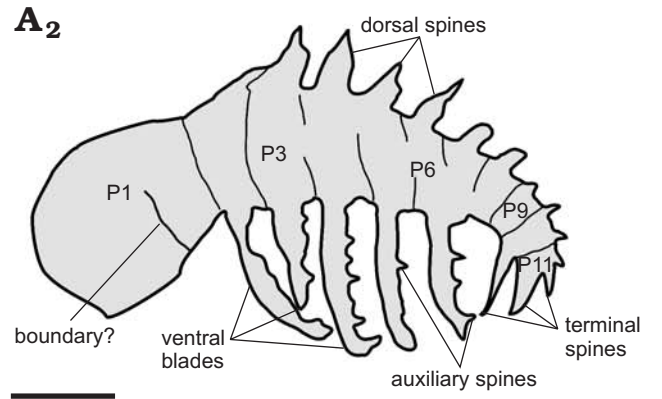
2017 *Stanleycaris hirpex* Caron, Gaines, Mángano, Streng, and Daley 2010; Pates et al. 2017: 620–624, figs. 3, 5, table 2.

Etymology: From the Latin *hirpex*, large rake; in reference to the morphology of the dorsal spines.

Type material: Holotype: ROM 59944. Paratypes: ROM 59975–77 all from the type locality.

Type locality: Stephen Formation (Cambrian Series 3, Stage 5), near Stanley Glacier (Kootenay National Park), British Columbia, Canada. GPS coordinates N51,10.781; W116,02.509 (Caron et al. 2010).

Type horizon: Claystone of cycle 5 (Caron et al. 2010: supplementary material 3B).



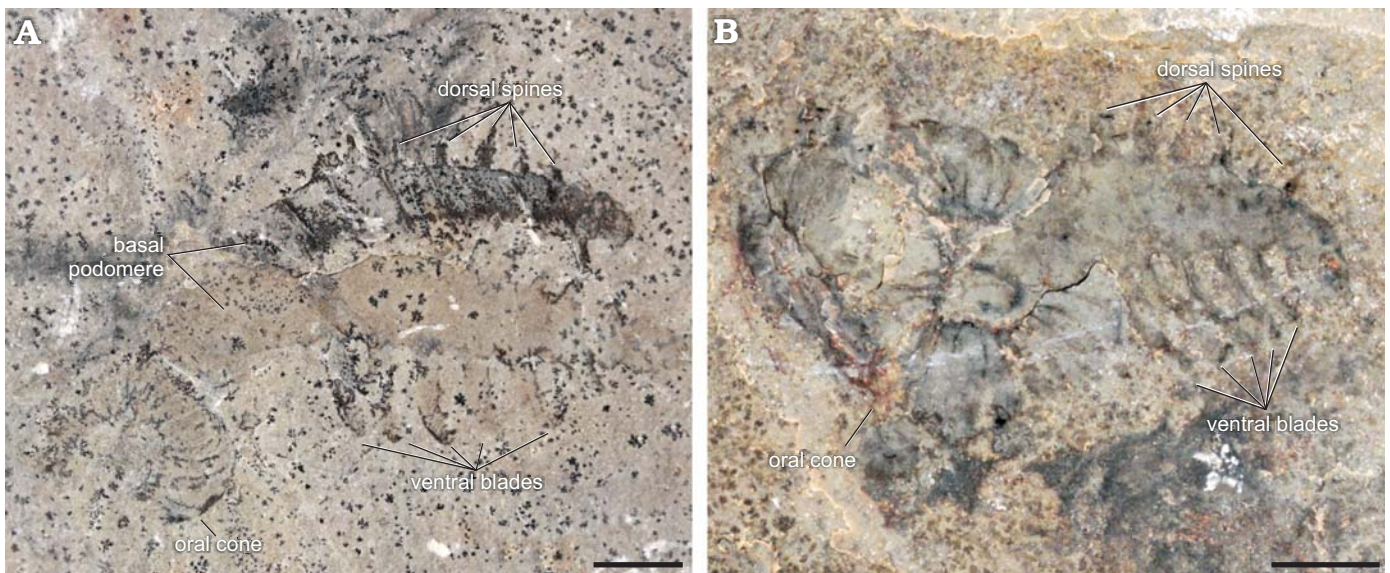


Fig. 2. The radiodontan *Stanleycaris hirpex* gen. et sp. nov. from the Stephen Formation (Cambrian Series 3, Stage 5), British Columbia, Canada. Frontal appendages associated with oral cones. **A.** Paratype, ROM 59976. **B.** Paratype, ROM 59977. Scale bars 5 mm.

Material.—37 specimens including 11 pairs of appendages and 11 assemblages with appendages, mouthparts and/or body segments in close proximity. All material from the type locality, stored at the ROM.

Diagnosis.—*Stanleycaris* with double-pointed dorsal spines on P2–6.

Description.—The lengths of the appendages is in the range 12.5–30.3 mm (mean = 20.6 mm, standard deviation = 3.0, $n = 21$), as measured along the dorsal midline from the proximal margin to the terminus. There is no evidence for discrete size classes. The appendage consists of at least 11 podomeres, with the most proximal rectangular podomere being at least as wide as the following three podomeres and possibly subdivided into two articles (boundary? in Fig. 1A, B). The appendage tapers in height from podomere 2 to the terminal end, with a convex curve along the dorsal margin. The distal region of the appendage is straight (Fig. 1B) or ventrally curved (Fig. 1A), with the terminal podomere rounded and bearing up to three terminal spines (Fig. 1A).

Robust dorsal spines project from the dorsal margin of podomeres 2–11 and are oriented vertically (Fig. 1B, C) or angled distally approximately 45° relative to the dorsal margin (distal podomeres in Fig. 1A). The largest dorsal spine is on podomere 2, where it can be as long as the width of the podomere (Fig. 1A, B), and the dorsal spines decrease in size along the length of the appendage towards the distal end. Dorsal spines are double-pointed on P2–6 but may be single-pointed on more distal podomeres (Fig. 1A, B).

Ventral blades project from podomeres 2–6, reaching a maximum length of 1.5 times the height of the podomere to which they attach (Fig. 1A). Ventral blades are straight (Fig. 1A) or slightly curved distally (Fig. 1B, C). As many as five single, straight auxiliary spines project perpendicularly from each ventral blade (Fig. 1A, B). Some specimens have a short, spineless ventral blade projecting from podomere 7 (Fig. 1B).

The appendages are often paired, and occasionally found as disarticulated assemblages with an oral cone in close proximity (Fig. 2). Oral cones are incomplete, but have a roughly circular or oval outline and a square central opening. Large and smaller plates can be distinguished in the oral cones, but their exact arrangements cannot be determined owing to incompleteness. The oral cones appear to have smooth outer margins that lack the subdivisions seen in the oral cone of *Anomalocaris canadensis* and the central margin shows no evidence of the extra rows of spiny plates of *Hurdia victoria*, making their overall configuration most similar to the oral cones of *Peytoia nathorsti* (Daley and Bergström 2012). Indistinct carapace material may be preserved in close association with the disarticulated assemblages (Fig. 2A).

Stratigraphic and geographic range.—Thin Stephen Formation (Cambrian Series 3, Stage 5), British Columbia, Canada (Caron et al. 2010).

Conclusions

The specimen of the putative lobopodian from the Valdemiedes Formation in Spain, previously referred to as “*Mureropodia*”, represents a frontal appendage of the radiodontan *Caryosyntrips*. The features put forward in support for the lobopodian affinity for “*Mureropodia*” by Gámez Vintaned and Zhuravlev (2018) are interpreted here as abiological artefacts including rock texture lineations and preparation marks. Instead, the specimen possesses a number of characters that indicate its euarthropod affinities as outlined above. The diversity and variability

← Fig. 1. The radiodontans *Stanleycaris hirpex* gen. et sp. nov. from the Stephen Formation (Cambrian Series 3, Stage 5), British Columbia, Canada (A–C) and *Stanleycaris* sp. from the Wheeler Formation (Cambrian Series 3, Drumian), Utah, USA. **A.** Holotype, ROM 59944. **B.** Paratype, ROM 59975, image mirrored in vertical axis. **C.** Paratype, ROM 59976. **D.** KUMIP 153923. P, podomere. Photographs (A₁–D₁), explanatory drawings (A₂–D₂). Scale bars 5 mm.

seen in radiodontans, both in terms of their morphology and their mode of preservation, is well documented and allows us to confidently associate incompletely or less well-preserved material, such as the present case, to well-known genera and species. Finally, we formalize *Stanleycaris* with the new ICZN-compliant taxon description included in this contribution.

Acknowledgements.—Specimens examined and figured in this study are hosted at the Royal Ontario Museum, Toronto, Ontario, Canada, and Division of Invertebrate Paleontology, Biodiversity Institute, University of Kansas, Lawrence, Kansas, USA, and we thank these institutions for access to the material. We also thank the editors Przemyslaw Gorzelak and Andrzej Kaim (both Institute of Paleobiology PAS, Warsaw, Poland), and the reviewer Bruce Lieberman (University of Kansas, Lawrence, USA), for comments and technical notes that improved the manuscript.

References

- Briggs, D.E.G. 1979. *Anomalocarisis*, the largest known Cambrian arthropod. *Palaeontology* 22: 631–633.
- Budd, G.E. 1997. Stem group arthropods from the Lower Cambrian Sirius Passet fauna of north Greenland. In: R. Fortey and R. Thomas (eds.), *Arthropod Relationships—Systematics Association Special Volume Series 55*, 125–138. Springer, Netherlands.
- Caron, J.-B., Gaines, R.R., Mángano, M.G., Streng, M., and Daley, A.C. 2010. A new Burgess Shale-type assemblage from the “thin” Stephen Formation of the southern Canadian Rockies. *Geology* 38: 811–814.
- Collins, D. 1996. The “evolution” of *Anomalocarisis* and its classification in the new arthropod class Dinocarida (nov.) and order Radiodonta (nov.). *Journal of Paleontology* 70: 280–293.
- Cong, P., Ma, X., Hou, X., Edgecombe, G.D., and Strausfield, N.J. 2014. Brain structure resolves the segmental affinity of anomalocaridid appendages. *Nature* 513: 538–542.
- Daley, A.C. and Bergström, J. 2012. The oral cone of *Anomalocarisis* is not a classic “peytoia”. *Naturwissenschaften* 99: 501–504.
- Daley, A.C. and Budd, G.E. 2010. New anomalocaridid appendages from the Burgess Shale, Canada. *Palaeontology* 53: 721–738.
- Daley, A.C. and Edgecombe, G.D. 2014. Morphology of *Anomalocarisis canadensis* from the Burgess Shale. *Journal of Paleontology* 88: 68–91.
- Daley, A.C. and Legg, D.A. 2015. A morphological and taxonomic appraisal of the oldest anomalocaridid from the lower Cambrian of Poland. *Geological Magazine* 152: 949–955.
- Daley, A.C., Budd, G.E., and Caron, J.-B. 2013. Morphology and systematics of the anomalocaridid arthropod *Hurdia* from the Middle Cambrian of British Columbia and Utah. *Journal of Systematic Palaeontology* 11: 743–787.
- Daley, A.C., Budd, G.E., Caron, J.-B., Edgecombe, G.D., and Collins, D. 2009. The Burgess Shale anomalocaridid *Hurdia* and its significance for early euarthropod evolution. *Science* 323: 1597–1600.
- Gaines, R.R. 2011. A new Burgess Shale-type locality in the “thin” Stephen Formation, Kootenay National Park, British Columbia: stratigraphic and paleoenvironmental setting. *Palaeontographica Canadiana* 31: 73–88.
- Gámez Vintaned, J.A. and Zhuravlev, A.Y. 2018. Comment on “*Ayshecia prolata* from the Utah Wheeler Formation (Drumian, Cambrian) is a frontal appendage of the radiodontan *Stanleycaris*” by Stephen Pates, Allison C. Daley, and Javier Ortega-Hernández. *Acta Palaeontologica Polonica* 63: 103–104.
- Stephen Pates [stephen.pates@zoo.ox.ac.uk], Department of Zoology, University of Oxford, Oxford, OX1 3PS, UK.
- Allison C. Daley [allison.daley@unil.ch], Institute of Earth Sciences, University of Lausanne, Géopolis, CH-1015, Lausanne, Switzerland.
- Javier Ortega-Hernández [jo314@cam.ac.uk], Department of Zoology, Downing Street, University of Cambridge, Cambridge, CB2 3EJ, UK.
- Gámez Vintaned, J.A., Liñán, E., and Zhuravlev, A.Y. 2011. A new early Cambrian lobopod-bearing animal (Murero, Spain) and the problem of the ecdysozoan early diversification. In: P. Pontarotti (ed.), *Evolutionary Biology—Concepts, Biodiversity, Macroevolution and Genome Evolution*, 193–219. Springer, Berlin.
- Haug, J.T., Mayer, G., Haug, C., and Briggs, D.E.G. 2012. A Carboniferous non-onychophoran lobopodian reveals long-term survival of a Cambrian morphotype. *Current Biology* 22: 1673–1675.
- Hou, X.-G., Bergström, J., and Ahlberg, P. 1995. *Anomalocarisis* and other large animals in the lower Cambrian Chengjiang Fauna of Southwest China. *GFF* 117: 163–183.
- ICZN (International Commission on Zoological Nomenclature) 2012. Amendment of Articles 8, 9, 10, 21, and 78 of the *International Code of Zoological Nomenclature* to expand and refine methods of publication. *Bulletin of Zoological Nomenclature* 69: 161–169.
- Lankester, E.R. 1904. The structure and classification of Arthropoda. *Quarterly Journal of Microscopical Science* 47: 523–582.
- Liu, Q. 2013. The first discovery of anomalocaridid appendages from the Balang Formation (Cambrian Series 2) in Hunan, China. *Alcheringa* 37: 338–343.
- Liu, J., Shu, D., Han, J., Zhang, Z.F., and Zhang, X.L. 2006. A large xenosid lobopod with complex appendages from the Chengjiang Lagerstätte (Lower Cambrian, China). *Acta Palaeontologica Polonica* 51: 215–222.
- Ortega-Hernández, J. 2015. Lobopodians. *Current Biology* 25: R873–875.
- Ou, Q., Liu, J., Shu, D., Han, J., Zhang, Z. Wan, X. and Lei, Q. 2011. A rare onychophoran-like lobopodian from the Lower Cambrian Chengjiang Lagerstätte, Southwestern China, and its phylogenetic implications. *JOURNAL OF PALEONTOLOGY* 85: 587–594.
- Ou, Q., Shu, D., and Mayer, G. 2012. Cambrian lobopodians and extant onychophorans provide new insights into early cephalization in Panarthropoda. *Nature Communications* 3: 1261.
- Pates, S. and Daley, A.C. 2017. *Caryosyntrips*: a radiodontan from the Cambrian of Spain, USA and Canada. *Papers in Palaeontology* 3: 461–470.
- Pates, S., Daley, A.C., and Lieberman, B.S. 2017a. Hurdid radiodontans from the middle Cambrian (Series 3) of Utah. *Journal of Paleontology* [published online].
- Pates, S., Daley, A.C., and Ortega-Hernández, J. 2017b. *Ayshecia prolata* from the Utah Wheeler Formation (Drumian, Cambrian) is a frontal appendage of the radiodontan *Stanleycaris*. *Acta Palaeontologica Polonica* 62: 619–625.
- Smith, M.R. and Ortega-Hernández, J. 2014. *Hallucigenia*’s onychophoran-like claws and the case for Tactopoda. *Nature* 512: 363–366.
- Van Roy, P., Daley, A.C., and Briggs, D.E.G. 2015. Anomalocaridid trunk limb homology revealed by a giant filter feeder with paired flaps. *Nature* 522: 77–80.
- Vinther, J., Stein, M., Longrich, N.R., and Harper, D.A. 2014. A suspension-feeding anomalocarid from the Early Cambrian. *Nature* 507: 496–499.
- Yang, J., Ortega-Hernández, J., Gerber, S., Butterfield, N.J., Hou, J.B., Lan, T., and Zhang, X.G., 2015. A superarmored lobopodian from the Cambrian of China and early disparity in the evolution of Onychophora. *Proceedings of the National Academy of Sciences of the USA* 112: 8678–8683.
- Young, F.J. and Vinther, J. 2017. Onychophoran-like myoanatomy of the Cambrian gilled lobopodian *Pambdelurion whittingtoni*. *Palaeontology* 60: 27–54.
- Zamora, S., Mayoral, E., Esteve, J., Gámez-Vintaned, J.A., and Santos, A. 2011. Exoskeletal abnormalities in paradoxid trilobites from the Cambrian of Spain, and a new type of bite trace. *Bulletin of Geosciences* 86: 665–673.

Received 14 November 2017, accepted 17 December 2017, available online 1 February 2018.

Copyright © 2018 S. Pates et al. This is an open-access article distributed under the terms of the Creative Commons Attribution License (for details please see <http://creativecommons.org/licenses/by/4.0/>), which permits unrestricted use, distribution, and reproduction in any medium, provided the original author and source are credited.